IOP Conf. Series: Materials Science and Engineering **1345** (2026) 012015 doi:10.1088/1757-899X/1345/1/012015

Measurement of Transverse Resistance for Stacks of Non-insulated REBCO Tapes

E Tamagnini[1*], E Barzi[2], A Zlobin[3], D Turrioni[3] and L Savoldi[1]

[1] MAHTEP Group, Energy Department, Politecnico di Torino, Torino, Italy
[2] Materials Science Department, The Ohio State University, Columbus, US
[3] Applied Physics and Superconducting Technology Directorate, Fermilab, Batavia, US

[*]E-mail: elena.tamagnini@studenti.polito.it

Abstract. Transverse resistance among adjacent conductors is a key parameter to calculate AC losses in superconducting cables with non-insulated conductors. The transverse pressure insert (TPI) previously developed and used at Fermilab was modified to measure transverse resistance of stacks made of non-insulated REBCO tapes as a function of transverse pressure at liquid nitrogen temperature. Pressure up to 322 MPa was applied with a hydraulic cylinder. A small current up to 10 A was flown in the stack sample through REBCO tape leads spliced above and below the stack. The latter had a bending radius larger than 6 mm to prevent the critical current degradation in REBCO leads. The voltage was measured just outside the compressed area. Stack samples included stacks of bare 4-mm wide REBCO tapes, as well as REBCO tapes alternated with 4-mm wide stainless-steel ribbons of 40 μm and 30 μm of thickness. We herein present the results of these transverse resistance measurements. Results show a stronger dependence on pressure for smaller pressure vs. larger ones. Also, of the two components of contact resistance, i.e. contact and bulk, the latter was negligible.

1. Introduction

Advancements in high-temperature superconducting (HTS) magnets are fueling interest in fusion energy research [1]. In tokamaks, for instance, large-scale magnets require high-current cables, often based on the Cable-in-Conduit Conductor (CICC) design, where REBCO tapes are embedded in a copper matrix [2]. However, for central solenoid (CS) magnets, an alternative involves winding HTS tapes directly into coils [3]. In such cases, a key design choice is whether to use insulated or non-insulated tapes.

Non-insulated REBCO tapes offer improved quench protection by allowing current to bypass local hot spots, but they also present drawbacks: notably, slower charging times and increased AC losses due to eddy currents flowing across the entire stack [4]. As a result, the transverse resistance of the HTS stack becomes a critical parameter for loss evaluation.

To address this, an experimental, exploratory campaign was conducted to measure the transverse resistance of a non-insulated (bare) HTS stack (Sample A), at 77 K, under applied pressures ranging from 10 MPa to 322 MPa, using a Transverse Pressure Insert (TPI). Two additional stacks, reinforced with alternating stainless-steel layers of 40 μm (Sample B) and 30 μm (Sample C) thickness respectively, were tested under the same conditions to assess the impact of mechanical reinforcement on electrical behaviour.

From the data, transverse resistivity was derived, useful for FEM simulations and tape comparison, along with estimations of contact resistance, including its bulk contribution, which was found negligible.

The following *Methods* section outlines the experimental setup, TPI modifications, and sample configurations. The *Results and Discussion* section presents resistance–pressure curves, of contact resistance R_C and transverse resistivity ρ_t, contact resistance bulk estimation, and a comparison across samples, summarized through plots.

2. Methods

2.1 Experimental procedure

Transverse resistance measurements of the stacks were carried out using a modified version of the Transverse Pressure Insert (TPI). After mounting the sample in the TPI, the apparatus was immersed in a liquid nitrogen bath at 77 K. An initial transverse pressure was then applied vertically to the stack in monotonic loading mode, using a 20-ton hydraulic cylinder mounted at the top of the device. Once the pressure had stabilized, a current ramp was applied to the stack, and the voltage was recorded via two voltage taps placed on the leads, using a dedicated data acquisition (DAQ) system. The measurement uncertainty for the resistance values is largely determined by the Agilent 6680A model used for the power supply. For currents between 0 and 20 A, the uncertainty on the measurement resistance is ±2.5%.

After each measurement, the current was stopped, the pressure was increased, and the measurement process (current ramp, voltage acquisition, and current stop) was repeated. Pressure was incrementally increased step by step until a maximum of 322 MPa was reached. Subsequently, the pressure was decreased stepwise, and the same measurement process was repeated at each level. The increasing-pressure phase is referred to as the "direct" loading, while the decreasing-pressure phase is called the "reverse" unloading. One complete "cycle" consists of both the direct and reverse phases. For each sample, three consecutive measurement cycles were performed.

For the first stack (bare-Sample A), the current was ramped up to 10 A, whereas for the second and third stacks (reinforced-Sample B and C), it was limited to 2 A. Voltage values were recorded throughout each current ramp at every pressure level during each cycle. With both voltage and current known, the transverse resistance R of the stack was calculated as the slope of the corresponding V-I curve at each pressure point.

2.2 TPI modifications

Although the TPI had been used in previous similar measurements [5] [6], specific modifications were necessary for this experiment. In particular, changes were made to the bottom section of the device. In earlier configurations, the sample was positioned inside a groove; for this study, however, the bottom plate was inverted to allow the sample to rest on a flat surface. The sample was then secured by wrapping it in Kapton and integrating additional elements, as detailed in this section.

A critical consideration is the minimum bending radius of REBCO tapes, which is 6 mm [7]. To accommodate this, a copper support for the stack, clearly illustrated in Figure 1a, was added to the bottom of the TPI. This support featured an internal radius of 6 mm (larger on the outer side, where the leads are placed) and was specifically designed to maintain its curvature under applied pressure.

The complete assembly process is depicted in Figure 1. It begins with the placement of the stack onto the pre-bent copper support (Figure 1a). Figures 1b and 1c show the addition of G-10, a high-pressure fiberglass laminate, which was used to hold the sample firmly in place. Figure 1d illustrates the insertion of a Kapton laminate between the stack and the bottom plate to provide electrical insulation.

In Figure 1e, the G-10 is shown shaped to accommodate the installation of the safety collars, which are presented in Figure 1f, where the TPI is shown sealed in the bottom, too. These two-piece shaft collars were clamped around the stack to ensure mechanical restraint and provide protection in the event of a stack ejection. Also visible in Figure 1f are the voltage taps, which were connected to the current leads soldered onto the REBCO tapes for voltage measurements.

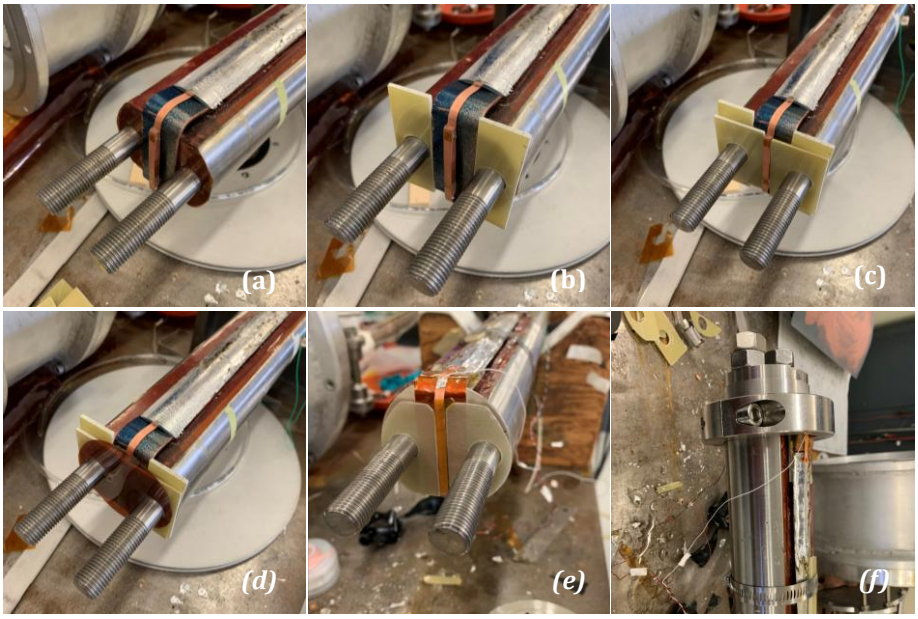

Figure 1. Steps for the TPI assembly. (a) Stack placed on the copper bent support; (b) G-10 added for bent support; (c) G-10 added for the stack; (d) Kapton laminate addition; (e) G-10 shaped; (f) bottom part secured with bolts and two-piece shaft collars.

2.3 Samples

Following the description of the experimental procedure and the TPI modifications, the focus now shifts to the samples themselves. Figure 2 provides a schematic representation of the stacks, with the direction of the applied pressure indicated by an arrow. Each REBCO tape is approximated as a central thin high-temperature superconducting layer (SC) encased in copper (Cu). Several key parameters are labelled in the figure: L denotes the tape length, w the tape width, t_{SC} the REBCO thickness, t_{SS} the stainless-steel tape thickness, and L_{eff} the effective contact length across the tape stack, which differs between the bare (left) and the reinforced stacks (right) in Figure 2. In the first case, L_{eff} is equal to the REBCO tape thickness, while in the reinforced cases it is equal to half REBCO tape thickness plus half stainless-steel thickness.

The figure specifically represents Sample A, the bare REBCO stack, on the left, and Samples B and C on the right, with the only difference being the alternating inclusion of stainless-steel tapes (SS) in place of REBCO tapes.

The schematic also highlights the contact points between adjacent tapes ("Contacts"), as well as the two ends of the tape stack ("Lead+" and "Lead−"), which are soldered to the TPI current leads. These are also the positions where the "Voltage taps", used for electrical measurements, are placed. The first sample, Sample A, consists of 16 SCS4050-AP REBCO tapes (SuperPower [7]), each featuring a 50 µm thick substrate and a 1.6 µm thick high-temperature superconducting (HTS) layer. The second (Sample B) and third (Sample C) stacks contain 10 REBCO tapes of the same specification, alternated with 9 stainless steel tapes.

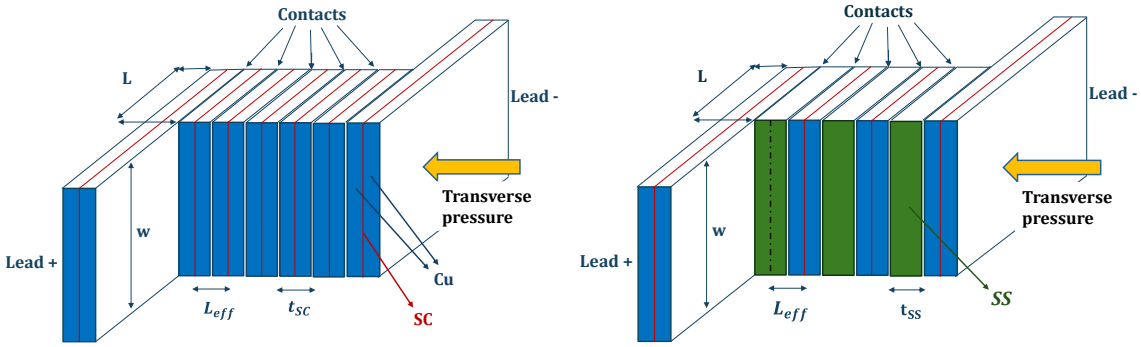

Figure 2. The bare sample (A) is on the left and the reinforced samples (B and C) are displayed on the right side of the figure.

It is important to note that for this type of REBCO wire, the critical current (I_C) at 77 K under self-field conditions is approximately 170 A [7]. Since the maximum current applied during the experiment was significantly lower, no superconducting-to-resistive transition was expected to occur within the stack during the current ramp.

Table 1 summarizes the dimensions of each tape used for the three samples (A, B, C).

Table 1. Tape dimensions. REBCO dimensions are the same for all samples, while the stainless-steel tapes changes in the sample B and sample C.

Type of tape	Length [mm]	Width [mm]	Thickness [mm]
REBCO- all samples (A, B, C)	47.75	4.03	0.07
Stainless steel- sample B	47.75	3.95	0.04
Stainless steel- sample C	47.80	4.13	0.03

3. Results and Discussion

3.1 Contact Resistance and Transverse Resistivity

As explained in the previous sections, the transverse resistance R of each stack has been measured through the experiment. Based on these measurements, it is possible to calculate the contact resistance R_C, given the number of contact interfaces N_C (in Sample A: N_C = 15, while in Sample B and C: N_C = 18), using the relation:

$$R_C = \frac{R}{N_C} \tag{1}$$

Once R_C , is known, the transverse resistivity ρ_t can be computed as:

$$\rho_t = R_C \frac{S_C}{L_{eff}} \tag{2}$$

Here, L_{eff} is the effective contact length, and S_c is the contact area, which corresponds to the tape width w multiplied by the tape length L, illustrated in Figure 2.

Considering Sample A, Figure 3 shows both contact resistance R_C and transverse resistivity ρ_t as functions of pressure. Since they differ only by constant geometric factors, they exhibit the same trend as transverse resistance R. For the sake of clarity, only the first and third measurement cycles are shown. The measurements start at 10 MPa, which corresponds to the initial pre-compression due to the TPI weight on the sample and extend up to a maximum pressure of 322 MPa. From the plot, it is evident that during both the loading (direct) and unloading (reverse) phases, the values decrease as pressure increases. Microscopically, this behaviour can be attributed to micro-plastic deformations occurring at the contact interfaces under pressure, which increase the effective contact area and thus reduce resistance. Additionally, for each cycle, the resistance during the unloading phase is consistently lower than during the loading phase.

Examining the end of each reverse phase (at 10 MPa), the resistance is found to be higher than at the beginning of the corresponding cycle. This increase may result from residual plastic deformation in the sample at high pressure, which slightly reduces the initial pre-compression and

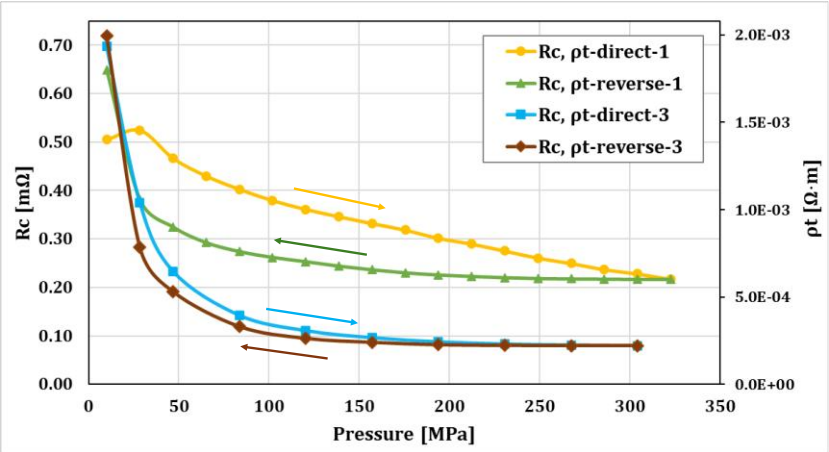

Figure 3. Sample A: contact resistance R_C and transverse resistivity ρ_t as a function of pressure.

leads to an increase in resistance. Notably, a step-like change in resistance is observed between the first and the third cycle. This could be due to irreversible micro-plastic deformations formed during the first cycle, which enhance the contact area permanently, leading to lower resistance in the subsequent cycles. Looking at plot in Figure 3, it can also be observed that both values tend to stabilize after three cycles, around 100 MPa.

Turning to the reinforced samples, Sample B and Sample C, the measurements of contact resistance and transverse resistivity for Sample B are presented in Figure 4, while those for Sample C are shown in Figure 5. The general behaviour of resistance and resistivity is qualitatively the same as that observed for Sample A.

Notably, the contact resistance R_C values are at least one orders of magnitude higher than those recorded for Sample A, reflecting the increased electrical resistance introduced by the reinforcement layers.

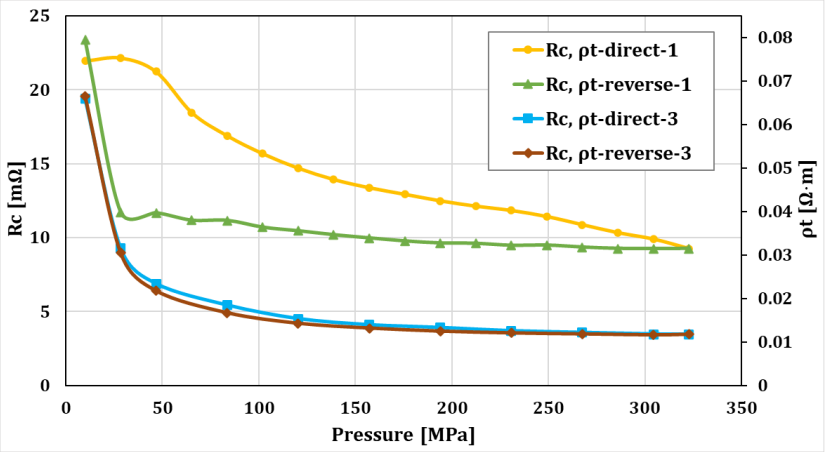

Figure 4. Sample B: contact resistance R_C and transverse resistivity ρ_t as a function of pressure.

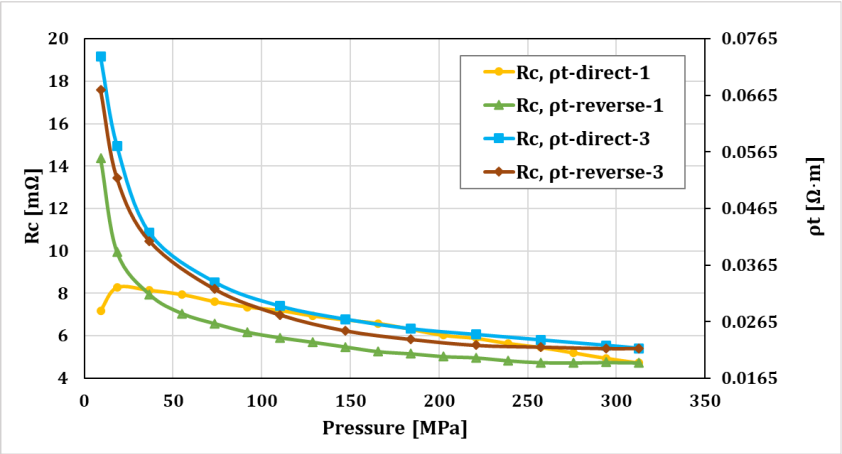

Figure 5. Sample C: contact resistance R_C and transverse resistivity ρ_t as a function of pressure.

3.2 Contact resistance-bulk estimation

The contact resistance, denoted as R_C, can be considered as the sum of its bulk components and the effective contact resistance between the tapes, $R_{C_{eff}}$.

The bulk components can be estimated and compared to the measured values of R_C. To explore this, it is possible to look at two extreme scenarios for the current path within each REBCO tape, shown in Figure 6. In the first scenario, we assume the buffer layers, which are inside the REBCO tape, as infinitely conductive, allowing current to flow through all layers of the tape. In the second scenario, the buffer layers are treated as insulators, which means the current can only travel through the external copper stabilizer.

In the first scenario, the bulk contributions to R_C are estimated to be around $10^{-10}\Omega$ for the copper layer, 10^{-8} Ω for the substrate, and 10^{-8} Ω for the stainless-steel layer (specifically for Samples B and C).

In the second scenario, the only bulk contribution comes from the external copper stabilizer at the edges of the tape, resulting in a resistance of about 10^{-6} Ω. These estimates clearly show that, in both scenarios, the total contact resistance R_C is primarily influenced by the effective contact resistance $R_{C_{eff}}$, with the bulk contributions being relatively insignificant. In fact, while the bulk resistances range from 10^{-10} to 10^{-6} Ω, the measured values of R_C are around 10^{-4} Ω for Sample A and 10^{-3} Ω for Sample B and Sample C.

We can further confirm the significance of $R_{C_{eff}}$, by looking at how R_C changes with pressure. This change indicates that better surface matching occurs under higher pressure, which leads to a decrease in contact resistance.

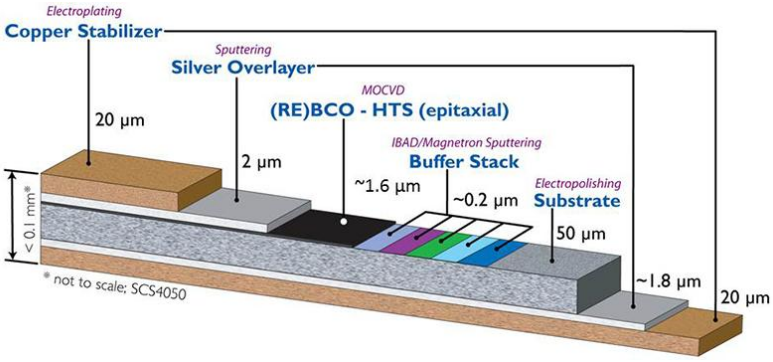

Figure 6. Schematic view of the layers of the REBCO tape [7].

3.3 Comparison and discussion

In conclusion, Figure 7 summarizes the contact resistance R_s results, where $R_s = R_C \cdot S_C$, as measured during the third cycle for all three samples (A, B, and C). As expected, the resistance values obtained for the reinforced stacks (Samples B and C) are at least one order of magnitude higher than those measured for the bare stack (Sample A).

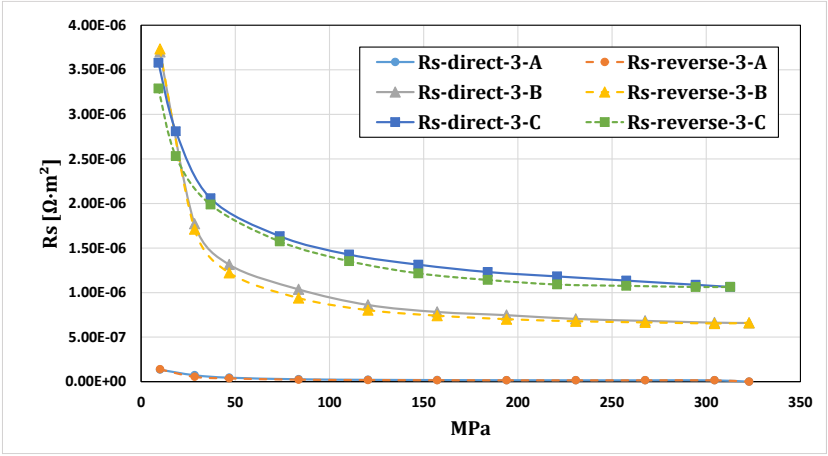

Figure 7. Comparison of contact resistance R_S [Ω m²] - Samples A, B and C.

Although a higher R_S would be expected for Sample B due to the greater thickness of its stainless-steel tapes, Sample C shows a higher resistance. This may be attributed to different surface conditions in the older stainless-steel tape used in Sample C. Given the exploratory nature of this study and the limited number of samples, no statistical analysis was performed and surface conditions were not controlled. As previously demonstrated, bulk contributions to R_S are negligible compared to the effective contact resistance $R_{C_{eff}}$, which is mainly determined by surface characteristics. The R_S results in Figure 7 were compared with those reported in [8], where applicable. For direct contact between REBCO tapes, the R_S range reported in [8] is 100–500 μΩ·cm^2. This is to be compared with the R_S value obtained for Sample A, which was 192 μΩ·cm^2, at 150 mPa.

4. Conclusions

The values presented in this work, particularly the transverse resistivity, can be directly applied in finite element method (FEM) simulations to model the electrical behaviour of high-temperature superconducting (HTS) assemblies. An ample range of pressure was used in the experiment to represent the varying levels of pressure in magnet systems operation.

For instance, in accelerator magnet systems, transverse resistivity values measured at pressures between 100 and 150 MPa are especially relevant, as these reflect typical operating conditions experienced by superconducting coils. At these pressure levels, the measured resistivity values are also found to be relatively stable and reliable.

As a potential next step, the experimental approach could be extended by introducing different interlayer materials between the REBCO tapes, in place of stainless steel, to investigate how alternative conductor compositions affect the overall contact and transverse resistance.

Acknowledgments

Elena Tamagnini thanks Allen Rusy for the preparation of the sample and for assistance with tests.

References

[1] Bruzzone P *et al.* 2018 High temperature superconductors for fusion magnets *Nucl. Fusion* **58** 103001.
[2] Zappatore A *et al.* 2019 A critical assessment of thermal–hydraulic modeling of HTS twisted-stacked-tape cable conductors for fusion applications *Supercond. Sci. Technol*. **32** 084004.
[3] Li Z Y *et al.* 2024 Development and construction of magnet system for world's first full high temperature superconducting tokamak Superconductivity **12** 100137.
[4] Wang Y and Song H 2016 Influence of turn-to-turn resistivity and coil geometrical size on charging characteristics of no-electrical-insulation REBCO pancake coils *Supercond. Sci. Technol*. **29** 075006.
[5] Barzi E Fratini M Zlobin A V 2002 A Device to Test Critical Current Sensitivity of Nb_3Sn Cables to Pressure *Advances in Cryogenic Engineering* **614** pp 45-52.
[6] Barzi E Turrioni D and Zlobin A V 2008 Effect of transverse pressure on brittle superconductors. *IEEE Trans. Appl. Sup* **18** pp 980-983.
[7] SuperPower Inc. 2G HTS Wire Specification n.d. Available at: https://www.superpower-inc.com/specification.aspx (accessed on 22 August 2025).
[8] Bonura M Barth C Joudrier A Troitino J F Fete A and Senatore C 2019 Systematic study of the contact resistance between rebco tapes: Pressure dependence in the case of no-insulation, metal co-winding and metal-insulation *IEEE Trans. Appl. Sup* **29**.